

Full-body Joint Trajectory Generation Using an Evolutionary Central Pattern Generator for Stable Bipedal Walking

Chang-Soo Park, Young-Dae Hong and Jong-Hwan Kim

Abstract—Central pattern generator (CPG) is used to control the locomotion of vertebrate and invertebrate animals, such as walking, running or swimming. It consists of biological neural networks that can produce coordinated rhythmic signals by using simple input signals. In this paper, a full-body joint trajectory generator is proposed for stable bipedal walking by using an evolutionary optimized CPG. Sensory feedback pathways are proposed in the CPG structure, which uses force sensing resistor (FSR) signals. In order to optimize the parameters of CPG, quantum-inspired evolutionary algorithm is employed. Then, controller is developed to control the position of both ankles and pelvis and the pitching angles of shoulders. The proposed trajectory generator controls the position of the center of pelvis along lateral direction, and the pitching angle of both shoulders in addition to the position of both ankles for stable biped locomotion. The stability of biped locomotion along lateral direction is improved by controlling the position of the center of pelvis along lateral direction. To reduce yawing momentum, the pitching angle of both shoulders are controlled. The effectiveness is demonstrated by simulations with the Webot model of a small-sized humanoid robot, HSR-IX and real experiments with HSR-IX.

I. INTRODUCTION

In spite of the complexity of high dimensional systems, many humanoid robots have been developed in these days and their performance has been very much improved [1]-[4]. Despite the improvement in hardware of humanoid robots, their control algorithms still need to be improved further to perform a practical task. In this regard, research on developing robust walking patterns of humanoid robots plays one of important roles in this field.

There are two typical approaches to generate robust walking patterns of humanoid robots: dynamic model based approach and biologically inspired approach. The former derives the equations of motion, which are utilized from mathematical model of robot, in the same way of conventional manipulator control [5], [6]. In the latter, one of popular schemes is to use central pattern generator (CPG). CPG consists of biological neural networks, which can endogenously produce multidimensional rhythmic signals. CPG is found both in vertebrate and invertebrate animals for the control of locomotion such as walking, running or swimming [7]-[9].

8-link simulated planar biped model based on the CPG was developed to generate each joint torque of humanoid robot's lower body [10], [11]. However, the walking pattern algorithm based on the CPG has two major problems. Firstly,

it requires much effort to generate appropriate oscillation signals for bipedal locomotion. To overcome this difficulty, the scheme which controls tip positions of legs in the Cartesian coordinate system, instead of trajectories of each joint, was presented [12]. Also, coupled adaptive oscillators, which can learn arbitrary periodic signals in a supervised learning framework, were suggested [13]. The first method is not sufficient to satisfy stable bipedal locomotion in 3D space, where the second method requires long time to learn involved parameters. The second major problem is that the walking pattern algorithm based on CPG is difficult to assign appropriate parameters for feedback pathways in neural oscillators. Thus, genetic algorithm or reinforcement learning were employed to optimize the involved parameters in neural oscillators [14], [15]. However, these methods require a great number of iterations to optimize parameters.

This paper proposes a full-body joint trajectory generation for stable bipedal locomotion based on evolutionary CPG. Neural oscillators for the CPG are developed to generate rhythmic signals. A controller is developed to control the position of both ankles and pelvis and the pitching angles of shoulders in Cartesian coordinate system using the CPG. It is easy to set up the involved parameters of the CPG for generation of appropriate output signals for bipedal locomotion. The proposed scheme controls the center position of pelvis along the lateral direction and the pitching angle of shoulders in addition to the position of ankles along the sagittal and vertical directions for stable bipedal locomotion in 3D space. Controlling the center position of pelvis along the lateral direction improves lateral stability, whereas controlling the pitching angle of shoulders reduces yawing momentum. The body posture for sensory feedback is obtained by using the signals of force sensing resistor (FSR) sensors attached to the sole of foot. In order to optimize the parameters of CPG, quantum-inspired evolutionary algorithm (QEA) is employed [16]. Effectiveness of the proposed scheme is demonstrated by computer simulations with the Webot model of a small-sized humanoid robot, HSR-IX and by real experiments with HSR-IX developed in the RIT Lab., KAIST.

This paper is organized as follows: In Section II, the neural oscillator is introduced to generate rhythmic signals and the evolutionary CPG is proposed. In Section III, simulation and experiment results are presented and finally concluding remarks follow in Section IV.

II. CPG-BASED CONTROL SCHEME

This section presents the proposed CPG-based control scheme, which consists of neural oscillators, for bipedal

The authors are with the Department of Electrical Engineering, KAIST, 335 Gwahak-ro, Yuseong-gu, Daejeon 305-701, Republic of Korea (e-mail: {cspark, ydhong, johkim}@rit.kaist.ac.kr).

locomotion. Then, the controller is developed to generate position trajectories of both ankles and the center of pelvis, and swinging trajectories of arms using the CPG. The body posture for sensory feedback is obtained using signals of FSR sensors attached to the sole of foot. The CPG has open parameters and they are optimized by the quantum-inspired evolutionary algorithm.

A. Neural Oscillator

The neural oscillator is biologically inspired to generate a rhythmic signal, which is defined as follows [17], [18]:

$$\tau \dot{u}_i = -u_i - \sum_{j=1}^N w_{ij} o_j - \beta v_i + u_0 + Feed_i \quad (1)$$

$$\tau' \dot{v}_i = -v_i + o_i \quad (2)$$

$$o_i = \max(0, u_i) \quad (3)$$

where u_i is the inner state of i th neuron, v_i is the self-inhibition state of i th neuron, u_0 is the input signal, o_i is the output signal, w_{ij} is the connecting weight between i th and j th neurons, τ and τ' are time constants, β is the weight of self-inhibition, and $Feed_i$ is the sensory feedback signal which is necessary for stable bipedal locomotion. Note that u_0 , τ , τ' and w_{ij} are constant parameters. τ and τ' have influence on the shape and frequency of output signal, u_0 affects the output amplitude and w_{ij} determine the phase difference between i th and j th neurons.

B. Application to Bipedal Locomotion of CPG

In the previous researches on CPG-based bipedal locomotion control, the controller generates each joint's torque or trajectory [10], [11], [13]. However, it is difficult to set the parameters of neural oscillators and the initial states that generate appropriate shape and frequency of output signal for bipedal locomotion. It is also difficult to design feedback pathways in the CPG. To solve these problems, in this paper, a controller is designed to generate the position trajectories of ankles and the center of pelvis in the Cartesian coordinate system, and swing trajectories of arms. The proposed method is simple to set up connecting weights in neural oscillators and the initial states of neurons, and to modify the step length or height. The controller is provided to control the positions of ankles and the center of pelvis and the pitching angle of shoulders.

The controller is provided to control the positions of left and right ankles along the sagittal direction as follows:

$$P_{L_X} = -A_X(o_1 - o_2) \quad (4)$$

$$P_{R_X} = A_X(o_1 - o_2) \quad (5)$$

where P_{L_X} and P_{R_X} are the distance from the center of pelvis to left and right ankles, respectively, along the sagittal direction (Fig. 1(a)). A_X is the amplitude scaling factor. By the above equations, the step length of humanoid robot becomes A_X .

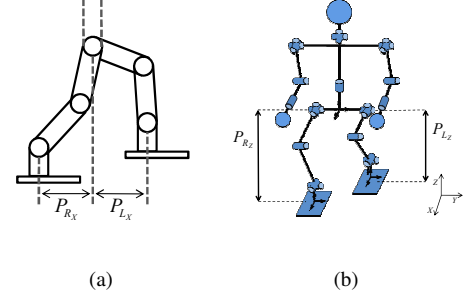


Fig. 1. The position of both ankles. (a) Along the sagittal direction. (b) Along the vertical direction.

The controller is provided to control the positions of left and right ankles along the vertical direction as follows:

$$P_{L_Z} = Z_c - A_Z(o_3 - o_4) \quad (6)$$

$$P_{R_Z} = Z_c + A_Z(o_3 - o_4) \quad (7)$$

where P_{L_Z} and P_{R_Z} are the distance from the center of pelvis to left and right ankles, respectively, along the vertical direction (Fig. 1(b)). Similarly, A_Z is the amplitude scaling factor. Note that the step height is determined as A_Z . Z_c is the offset factor, which is equivalent to the height of pelvis when the humanoid robot is in double support phase.

The projected ankle trajectories on X-Z plane can be approximated as semi-ellipsoid. Thus, the desired phase difference between ankle's vertical and horizontal oscillations should be $\pi/2$ [12]. If bipedal locomotion is only simulated in 2D space, it is sufficient to consider positions along the sagittal and the vertical directions for stable bipedal locomotion. In 3D space, however, positions along the lateral direction in addition to sagittal and vertical directions have to be considered for stable bipedal locomotion. Therefore, position control of the center of pelvis along the lateral direction should be added to the controller. The following controller is provided to control the center position of pelvis along the lateral direction:

$$P_{COP_Y} = A_Y(o_5 - o_6) \quad (8)$$

where P_{COP_Y} is the distance between the center of pelvis and the center position of both ankles along the lateral direction (Fig. 2). In order to make a humanoid robot stable along the lateral direction, the lateral position of the center of pelvis should be always maintained to be the position of supporting leg. However, this condition is practically impossible because supporting leg changes periodically. To solve this problem, the distance between the supporting leg and the center of pelvis along the lateral direction is controlled using a neural oscillator.

When humanoid robot is double support, the center position of pelvis is given as the center position of both ankles along the lateral direction. When P_Z increases, the distance between the center of pelvis and the supporting leg decreases

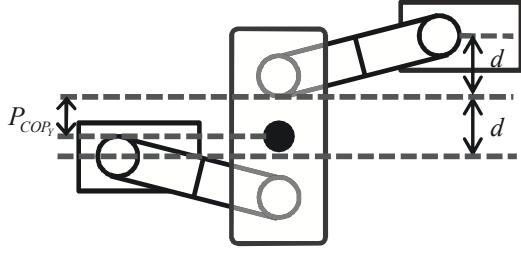


Fig. 2. The position of the center of pelvis along the lateral direction.

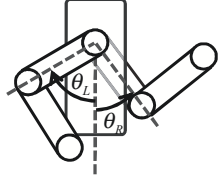


Fig. 3. The pitching angle of both shoulders.

such that P_{COF_Y} increases. When P_Z is maximum, the distance between the center of pelvis and the supporting leg becomes minimum, which makes P_{COF_Y} maximum as well. On the other hand, when P_Z decreases, the distance between the center of pelvis and the supporting leg increases such that P_{COF_Y} decreases. Consequently, the phase difference between P_Z and P_{COF_Y} becomes zero.

When walking speed increases, humanoid robot may slip due to yawing moment. To compensate for the yawing moment, arm swinging motion should be provided. The following controller is to control the pitching angles of left and right shoulders:

$$\theta_L = A_\theta(o_7 - o_8) \quad (9)$$

$$\theta_R = -A_\theta(o_7 - o_8) \quad (10)$$

where θ_L and θ_R are the pitching angle of left and right shoulders, respectively (Fig. 3). The resulting yawing moment can be approximated as follows:

$$|T| = |m_L D_L \ddot{x}_L + J_P \ddot{\theta}_P + m_P D_P \ddot{x}_P + m_A D_{A1} \ddot{x}_{A1} - m_A D_{A2} \ddot{x}_{A2}| \quad (11)$$

where m_L , m_P and m_A are the mass of each leg, body and each arm, respectively, \ddot{x}_L , \ddot{x}_P , \ddot{x}_{A1} and \ddot{x}_{A2} are the acceleration of swing leg, body, and each arm, respectively, along sagittal direction, θ_P is the yawing angle acceleration of body and D_L , D_P , D_{A1} and D_{A2} are the distance of swing leg, body, and each arm, respectively, and supporting leg along lateral direction (Fig. 4). $|x_L|$ and $|x_P|$ are defined as $|2A_X(o_1 - o_2)|$ and $|A_X(o_1 - o_2)|$, respectively. Then, $\ddot{x}_P = 0.5\ddot{x}_L$, and $\ddot{x}_{A2} = -\ddot{x}_{A1}$, as $\theta_L = -\theta_R$. Accordingly, the yawing moment can be approximated as

$$|T| = |\ddot{x}_L(m_L D_L + 0.5m_P D_P) + J_P \ddot{\theta}_P + m_A \ddot{x}_{A1}(D_{A1} + D_{A2})|. \quad (12)$$

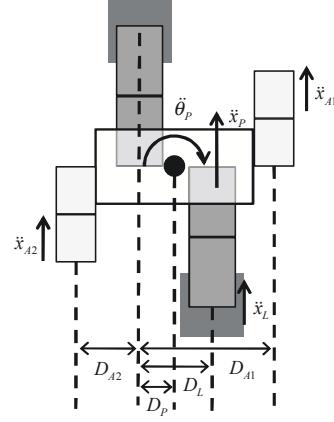


Fig. 4. The yawing moment.

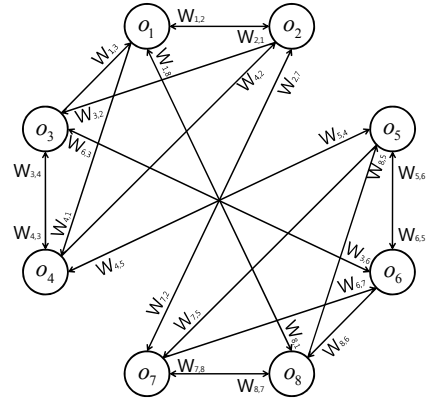


Fig. 5. The neural oscillator.

Note that when \ddot{x}_L increases, \ddot{x}_{A1} decreases and also when \ddot{x}_L decreases, \ddot{x}_{A1} increases. Thus, as the phase difference of \ddot{x}_{A1} and \ddot{x}_{A1} is π , the phase difference of P_x and θ_{Arm} becomes π .

Neural oscillators are designed for stable bipedal locomotion as shown in Fig. 5 and the connecting weights are set to satisfy the phase difference conditions derived in this section as shown in Table. I.

C. Sensory Feedback Design

Sensory feedback pathways are designed to maintain humanoid robot's balance and to prevent it from falling down to the ground. To maintain the balance, information related to humanoid robot's body posture is needed such that four FSR sensors are attached to the sole of each foot. The body posture along the vertical direction is obtained using the difference between left foot's vertical reaction force, F_L , and right foot's vertical reaction force, F_R . The body posture along the sagittal direction can be obtained using $F_{L_f} - F_{L_b}$ and $F_{R_f} - F_{R_b}$, where F_{L_f} , F_{R_f} , F_{L_b} and F_{R_b} are left and right foot's front and back vertical reaction forces, respectively. The body posture along the lateral direction is obtained using $F_{L_l} - F_{L_r}$ and $F_{R_l} - F_{R_r}$, where F_{L_l} , F_{R_l} , F_{L_r} and F_{R_r} are left and right foot's left and right vertical

TABLE I
CONNECTING WEIGHTS

$w_{1,2}$	1.5	$w_{2,1}$	1.5	$w_{3,4}$	1.5	$w_{4,3}$	1.5
$w_{5,6}$	1.5	$w_{6,5}$	1.5	$w_{7,8}$	1.5	$w_{8,7}$	1.5
$w_{1,4}$	0.5	$w_{4,1}$	0.5	$w_{2,3}$	0.5	$w_{3,2}$	0.5
$w_{5,8}$	0.5	$w_{8,5}$	0.5	$w_{6,7}$	0.5	$w_{7,6}$	0.5
$w_{1,6}$	0.5	$w_{5,1}$	0.5	$w_{5,2}$	0.5	$w_{2,6}$	0.5
$w_{3,7}$	0.5	$w_{8,3}$	0.5	$w_{8,4}$	0.5	$w_{4,7}$	0.5

reaction force, respectively.

The sensory feedback pathways are defined as follows:

$$Feed_1 = k_1((F_{L_f} - F_{L_b}) - (F_{R_f} - F_{R_b})) \quad (13)$$

$$Feed_2 = -Feed_1 \quad (14)$$

$$Feed_3 = k_2(F_L - F_R) + k_3((F_{L_l} - F_{L_r}) + (F_{R_l} - F_{R_r})) \quad (15)$$

$$Feed_4 = -Feed_3 \quad (16)$$

$$Feed_5 = k_4(F_L - F_R) + k_5((F_{L_l} - F_{L_r}) + (F_{R_l} - F_{R_r})) \quad (17)$$

$$Feed_6 = -Feed_5. \quad (18)$$

Since $Feed_1$ and $Feed_2$ modulate the position of both ankles and body along the sagittal direction, $(F_{L_f} - F_{L_b})$ and $(F_{R_f} - F_{R_b})$, which are related to the body posture along the sagittal direction, are considered in (13) and (14). $Feed_3$ and $Feed_4$ modulate the position of both ankles and body along the vertical direction, so $(F_L - F_R)$, which is related to the body posture along the vertical direction, are considered in (15) and (16). $Feed_5$ and $Feed_6$ modulate the position of the center of pelvis along the lateral direction, so $(F_{L_l} - F_{L_r})$ and $(F_{R_l} - F_{R_r})$, which are related to the body posture along the lateral direction, are considered in (17) and (18). Also $(o_3 - o_4)$ and $(o_5 - o_6)$ are in phase, so $(Feed_3 - Feed_4)$ and $(Feed_5 - Feed_6)$ are satisfied in phase. Therefore, $(F_{L_l} - F_{L_r})$ and $(F_{R_l} - F_{R_r})$ should be considered in calculating $Feed_3$ and $Feed_4$. Similarly, also $(F_L - F_R)$ should be also considered in calculating $Feed_5$ and $Feed_6$.

D. Evolutionary Optimization for CPG algorithm

The proposed CPG controller has 11 parameters which consist of amplitude and feedback scaling factors and time constants. In this paper, these parameters are optimized by quantum-inspired evolutionary algorithm (QEA) [16]. QEA can explore the search space with a smaller number of individuals and exploit the search space for a global solution within a short span of time. QEA is based on the concept and principles of quantum computing, such as the quantum bit and the superposition of states.

The key objectives in optimizing the parameters are to make the humanoid robot approach the goal as quickly as possible and to maintain its balance as stable as possible. Considering these objectives, the objective function is defined as follows:

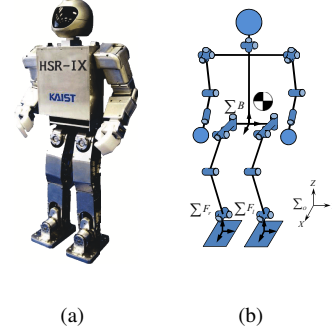


Fig. 6. Humanoid robot. (a) HSR-IX. (b) Configuration.

$$f = \frac{k_x T_1}{d|_{t=T_1}} + k_y \sum_{T=0}^{T_1} |P_{err}[T]| + k_\theta \sum_{T=0}^{T_1} |\theta_{err}[T]| + B_P \quad (19)$$

where $T_1/d|_{t=T_1}$ is the inverse proportion to velocity of bipedal locomotion for T_1 , $\sum_{T=0}^{T_1} |P_{err}[T]|$ is the sum of position error along the lateral direction for T_1 , and $\sum_{T=0}^{T_1} |\theta_{err}[T]|$ is the sum of angle error along the yawing direction for T_1 . k_x , k_y and k_θ are constants. The first term corresponds to the objective function for fast bipedal locomotion. The second term corresponds to the objective function for decreasing position error along the lateral direction. The third corresponds to the objective function for decreasing pelvis angle error along the yawing direction. The last is the penalty which is to be given if humanoid robot loses its balance and collapses, where B_P is assigned a priori as a constant value.

III. SIMULATIONS AND EXPERIMENT

The effectiveness of the proposed algorithm was demonstrated by computer simulations with the Webot model of a small sized humanoid robot, HSR-IX and by real experiment with HSR-IX (Fig. 6(a)) [4]. HSR-IX is the latest one of HSR-series. HSR is a small-sized humanoid robot that has been continuously undergoing redesign and development in RIT Lab, KAIST since 2,000. Its height and weight are 52.8cm and 5.5kg, respectively. It has 26 DOFs that consists of 14 RC servo motors in the upper body and 12 DC motors with harmonic drive for reduction gears in the lower body (Fig. 6(b)). In each simulation, if humanoid robot walks n steps without falling down to the ground in bipedal locomotion and n is lower than 15, the total number of steps is n , else the total number of steps is 15. $\tau/\tau' = 0.105/0.132$ and $\tau = 0.105A_\tau$ were used. The parameters in the CPG were optimized by QEA.

A. Simulation Results Including Position Control along the Lateral Direction

The controller is provided to control the position of the center of pelvis along the lateral direction for increasing

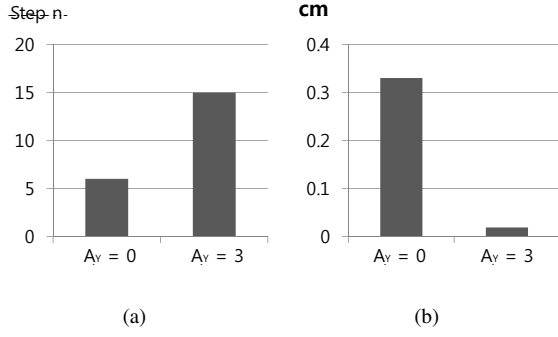


Fig. 7. Simulation results including position control along the lateral position. (a) The total number of steps. (b) The position error along the lateral direction.

stability along the lateral direction. Fig. 7 shows a comparison result between controlling the position of left and right ankles, respectively, along the sagittal and vertical directions ($A_Y = 0$) and controlling the position of the center of pelvis along the lateral direction ($A_Y = 3$) in addition to the position of left and right ankles, respectively, along the sagittal and vertical directions (Videos 1 and 2). $A_X = 2.0$, $A_\tau = 1.5$ and $A_Z = 1.2$ were used. In the former case, i.e. when $A_y = 0$, the position of the center of pelvis along the lateral direction was constant such that there is no lateral motion for balancing to be stable. In the latter case with $A_Y = 3$, the total number of steps increased and the position error along the lateral direction defined in (19) decreased. This result illustrates that it improves stability of bipedal locomotion if the controller controls the position of the center of pelvis along the lateral direction in addition to the position of ankles along the sagittal and vertical directions.

B. Simulation Results Including Sensory Feedback Pathways

The sensory feedback pathways in the CPG maintain humanoid robot's balance and prevent it from falling down to the ground. In this paper, the sensory feedback pathways were designed by FSR signals. Fig. 8 shows the effect of including sensory feedback pathways. $A_X = 3.0$, $A_\tau = 1.5$ and $A_Z = 1.2$ were used (Videos 3 and 4). The parameters in sensory feedback pathways were evolutionary optimized by QEA. In this simulation, humanoid robot's walking speed was faster than that in Section.III-A, such that it was hard to maintain balance without sensory feedback pathways. Controlling the position with sensory feedback pathways, the total number of steps increased and the position error along the lateral direction decreased. This result illustrates that sensory feedback based on FSR sensor maintains humanoid robot's balance and prevents it from falling down to the ground.

C. Simulation Results of Evolutionary Optimization

The proposed algorithm has 11 parameters. These parameters were evolutionary optimized by QEA. In Fig. 9, the velocity, the position error along the lateral direction and angle error along the yawing direction are plotted, when k_x

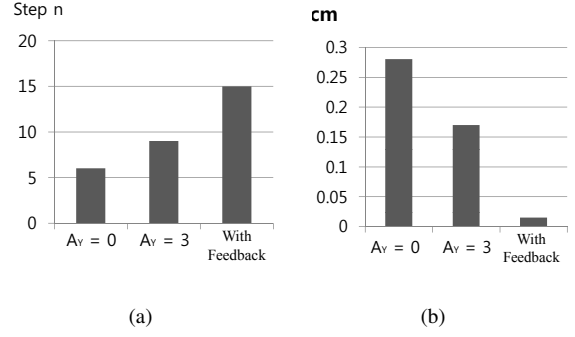


Fig. 8. Simulation results including sensory feedback pathways. (a) The total number of steps. (b) The position error along the lateral direction.

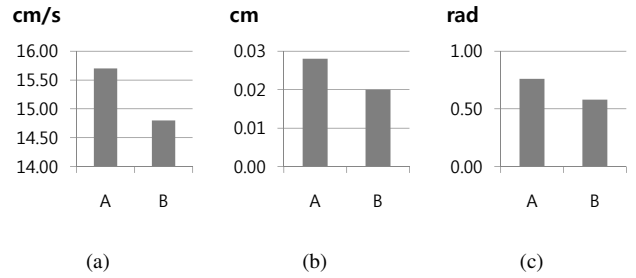


Fig. 9. Simulation results of evolutionary optimization. A is with $k_x = 500$, $k_y = k_\theta = 100$ and B is with $k_x = 500$, $k_y = k_\theta = 200$. (a) The velocity. (b) The position error along the lateral direction. (c) The angle error along the yawing direction.

was fixed as 500 and k_y and k_θ , 100 and 200 (Videos 5 and 6). When k_y and k_θ increased, the walking velocity was slower, but the position error along the lateral direction and the angle error along the yawing direction decreased. This result illustrates that when k_y and k_θ decrease, optimization of the parameters make the humanoid robot walk faster, whereas when k_y and k_θ increase the optimization of the parameters make the bipedal locomotion more stable.

D. Simulation Results Including Swing Motion of Arms

The proposed controller controls the pitching angle of left and right shoulders, respectively, to compensate for the yawing moment. In Fig. 10, the yawing moments are plotted, when amplitude scaling factor of the pitching angle of shoulders, A_θ , was changed (Videos 7 and 8). As shown in Fig. 10, the yawing moment decreased, when A_θ increased. When $A_\theta = 1.0$, the yawing moment decreased by 8.8 percent over $A_\theta = 0.0$. This result illustrates that the yawing moment can be decreased by swinging along pitching direction.

E. Experiment Result

Experiment was carried out with the actual humanoid robot, HSR-IX. $\tau/\tau' = 0.105/0.132$, $\tau = 0.105A_\tau$, $A_\tau = 4$, $A_x = 2.0$, $A_y = 3.0$ and $A_z = 0.5$ were used. For stable bipedal locomotion in real experiment, the parameters, $k_1 \sim$

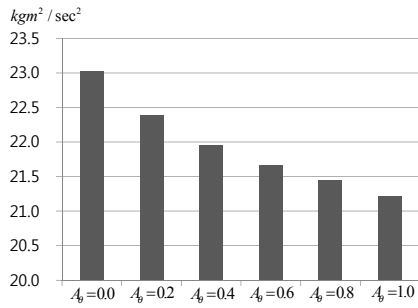


Fig. 10. The yawing moment including swing motion of arms.

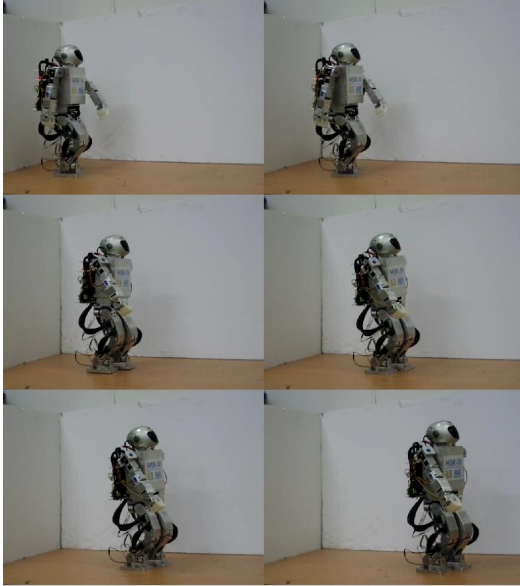


Fig. 11. Experiment result with evolutionary optimized CPG.

k_5 , in sensory feedback pathways of the CPG, were evolutionary optimized using the computer simulation of HSR-IX model by Webot. Then these parameters were slightly tuned for proper walking by trial and error in real experiment. As shown in Fig. 11, the humanoid robot achieved stable walking (Video 9).

IV. CONCLUSION

This paper proposed the full-body joint trajectory generation for stable biped locomotion based on evolutionary CPG. The neural oscillators in the CPG were developed to generate rhythmic signals. The proposed controller controlled the position of left and right ankles along both sagittal and vertical directions. In addition, it controlled the center position of pelvis along lateral direction and the pitching angles of both left and right shoulders. Also, the proposed controller generated the ankle trajectories along both sagittal and vertical directions using the CPG for stable biped locomotion in 3D space. The sensory feedback pathways in the CPG were designed by using FSR signals. The parameters in the CPG were optimized by using quantum-inspired evolutionary algorithm (QEA) for stable and fast biped locomotion. In order to demonstrate the performance

of the proposed scheme, computer simulations were carried out with the Webot model of the small sized humanoid robot, HSR-IX and real experiment was carried out with HSR-IX developed at the RIT Lab., KAIST.

V. ACKNOWLEDGMENTS

This research was supported by Basic Science Research Program through the National Research Foundation of Korea (NRF) funded by the Ministry of Education, Science and Technology (2010-0000831).

REFERENCES

- [1] K. Hirai, M. Hirose, Y. Haikawa, T. Takenaka, "The development of honda humanoid robot", in *Proc. IEEE Int. Conf. Robotics and Automations*, May 1998, pp. 1321–1326.
- [2] K. Akachi, K. Kaneko, N. Kanehiro, S. Ota, G. Miyamori, M. Hirata, S. Kajita, F. Kanehiro, "Development of humanoid robot HRP-3P," in *Proc. IEEE-RAS Int. Conf. Humanoid Robots*, Dec. 2005, pp. 50–55.
- [3] I.-W. Park, J.-Y. Kim, J. Lee, J.-H. Oh, "Online free walking trajectory generation for biped humanoid robot KHR-3(HUBO)," in *Proc. IEEE Int. Conf. Robotics and Automations*, May 2006, pp. 1231–1236.
- [4] J.-K. Yoo, B.-J. Lee and J.-H. Kim, "Recent Progress and Development of Humanoid Robot HanSaRam," *Robotics and Autonomous Systems*, vol. 57, no. 10, pp. 973–981, Oct. 2009.
- [5] S. Kajita, F. Kanehiro, K. Kaneko, K. Fujiwara, K. Yokoi, and H. Hirukawa, "A Realtime Pattern Generator for Biped Walking," in *Proc. IEEE Int. Conf. Robotics and Automation*, May 2002, pp. 31–37.
- [6] B.-J. Lee, D. Stonier, Y.-D. Kim, J.-K. Yoo and J.-H. Kim, "Modifiable Walking Pattern of a Humanoid Robot by Using Allowable ZMP Variation," *IEEE Trans. Robotics*, vol. 24, no. 4, pp. 917–925, Aug. 2008.
- [7] T. McMahon, "Muscles, Reflexes, and Locomotion," Princeton, NJ, Princeton University Press, 1984.
- [8] G. N. Orlovsky, T. Deliagina, and S. Grillner, "Neuronal Control of Locomotion: From Mollusc to Man," Oxford, Oxford University Press, 1999.
- [9] S. Grillner, T. Deliagina, A. El Manira, R. H. Hill, G. N. Orlovsky and P. Wallen, "Neural networks that co-ordinate locomotion and body orientation in lamprey," *Trends in NeuroSciences*, vol.18, no.6, pp. 270–279, 1995.
- [10] G. Taga, "Emergence of bipedal locomotion through entrainment among the neuro-musculo-skeletal system and the environment, *Physica D: Nonlinear Phenomena*, vol. 75, no. 1.3, pp. 190–208, 1994.
- [11] G. Taga, "A model of the neuro-musculo-skeletal system for human locomotion," *Biol Cybern*, vol. 73, pp.97–111, 1995.
- [12] Gen Endo, Jun Morimoto, Takamitsu Matsubara, Jun Nakanishi and Gordon Cheng, "Learning CPG Sensory Feedback with Policy Gradient for Biped Locomotion for a Full-body Humanoid," *the 20th national conference on Artificial intelligence*, Jul. 2005, pp. 1267–1273.
- [13] L. Righetti and A. J. Ijspeert, "Programmable Central Pattern Generators: an application to biped locomotion control," in *Proc. IEEE Int. Conf. Robotics and Automation*, May 2006, pp. 1585–1590.
- [14] K. Hase, and N. Yamazaki, "Computer simulation of the ontogeny of biped walking," *Anthropological Science*, vol. 106, no. 4 pp. 327–347, 1998.
- [15] T. Mori, Y. Nakamura, M.Sato, and S. Ishii, "Reinforcement learning for a cpg-driven biped robot," *Nineteenth National Conference on Artificial Intelligence*, Jul. 2004, pp. 623–630.
- [16] K.-H. Han and J.-H Kim, "Quantum-inspired evolutionary algorithm for a class of combinatorial optimization," *IEEE Trans. Evolutionary Computation*, vol. 6, pp. 580–593, 2002.
- [17] K. Matsuoka, "Sustained oscillations generated by mutually inhibiting neurons with adaptation," *Biol Cybern*, vol. 52, no. 6, 367–376, October. 1985.
- [18] K. Matsuoka, "Mechanisms of frequency and pattern control in the neural rhythm generators," *Biol Cybern*, vol. 56, no. 5, pp. 345–353, Jul. 1987.